Changing Functional Connectivity in the Child's Developing Brain Affected by Ischaemic Stroke

Roxane Licandro[1,2], Karl-Heinz Nenning[2], Ernst Schwartz[2], Kathrin Kollndorfer[2], Lisa Bartha-Doering[3], Georg Langs[2]
licandro@caa.tuwien.ac.at

[1]Institute of Computer Aided Automation - Computer Vision Lab, Vienna University of Technology; [2]Department of Biomedical Imaging and Image-guided Therapy - Computational Imaging Research Lab, Medical University of Vienna; [3]Department of Pediatrics and Adolescent Medicine, Medical University of Vienna

Abstract. Group studies using resting state functional Magnetic Resonance Imaging (rs-fMRI) enable the analysis of spatial and temporal brain signal correlations, independent of a specific stimulus. Here, we assess adaptive brain plasticity in developing resting state networks after ischaemic stroke of children between 7 and 17 years. We analyse long range and short range connectivity patterns during ageing using a graph representation and corresponding measurements. The evaluation is performed using rs-fMRI data of 16 control subjects and 16 stroke patients with corresponding psychological tests. The developing functional connectivity affected by ischaemic stroke exhibits significant differences to the control cohort. This suggests an influence of regenerating plasticity on short range long range connectivity changes, degree distribution and specific brain areas over age.

1 Introduction

Brain development starts in utero and continues during childhood together with cognitive maturation. While we understand parts of the functional organization in adults, our knowledge of its emergence during maturation is still limited. The development of its connectivity architecture is particularly interesting, since we suspect that it has a major role connected to our cognitive capabilities. Here, we present results quantifying the development of the connectivity architecture as observed in 16 children with normal development, and 16 children suffering from ischaemic stroke. We investigate the normal development of connectivity characteristics, and quantify the deviation from this development common to stroke patients. Structural changes of brain morphology and functional organisation can be measured with Magnetic Resonance Imaging (MRI) and functional MRI techniques (fMRI) [3][12]. Pediatric fMRI enables imaging neural activation of the child's brain corresponding to certain stimuli or tasks in a non-invasive way [1]. The rs-fMRI technique is able to reliably assess large-scale brain networks of healthy children longitudinally across the temporal, spatial and frequency domains [16].

Challenges and Motivation The challenge of longitudinal studies among children to identify functional connectivity is induced by the age and developmental related changes of the brain triggered by learning and experience (natural plasticity)[2], but also by pathology related modifications, and functional and structural reorganisation (adaptive plasticity) of brain tissue [11]. After a damage, plasticity and vulnerability of the brain influence recovery together with the injuries severity, the age and the time since damage [2]. Resting state fMRI enables the study of these processes driving the functional and structural organisation. Ultimately they can lead to improved functional outcome of children suffering from brain injuries, by developing novel interventional techniques or adapting therapy, dependent on the developmental stage of a disease [11].

Related Work Fair et al. [5] and Supekar et al. [15] use graph based analysis (e.g. path-length, hierarchy, clustering-coefficient and regional connectivity) of rs-fMRI data of the child's healthy brain and demonstrate an increase of long-range connectivity and a lower scattering of local connectivity during the development of the central nervous system in the child's healthy brain. Supekar et al. [15] observe that children have a similar global (small-world) organisation of the brain, but show differences in interregional connectivities and the hierarchy of organisation. Gordon et al. [8] apply ICA on Diffusion Tensor Imaging (DTI) and rs-fMRI data of children between 7 and 13 to identify resting state networks.

Contribution We analyse the development and modification of resting state connectivity networks in the pediatric brain after stroke between 7 and 17 years. We analyse adaptive plasticity and the relations to the developing connectivity networks in the healthy brain using Pearson correlation coefficient and graph based measures [13] of brain signals. We hypothesize that adaptive plasticity processes after stroke influence the formation of long range (LR) and short range (SR) connectivity over age, related to re-organisational processes and development of brain lesions after stroke [2]. Sepulcre et al. [14] compute the local and distant degree and physical distance between correlating regions in adults. They observe a strong local connectivity in the motor area, primary sensory area and strong distant connectivity in regions of high-order cognitive functions (attentional, memory and language processing). We adapted these measures for the child's brain for analysing the influence of stroke on the distribution of short and long range connectivity over age.

The data acquisition and preprocessing setup are summarised in Section 2. The evaluation setup and computed results are documented in Section 3 and a discussion and possibilities for future work are given in Section 4.

2 Methodology

Data acquisition: The participants in this study are 32 children between 7 and 17 years consisting of 16 control cases and 16 ischaemic stroke cases. The

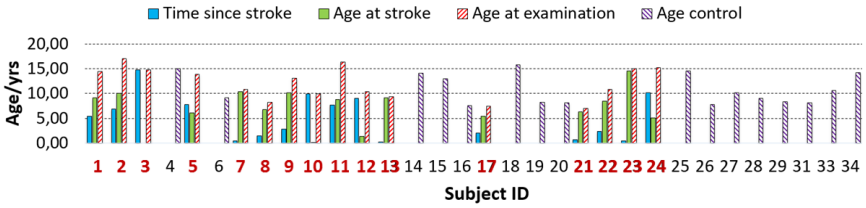

Fig. 1: Distribution of data: For every control subject we show age, for stroke patients, we show age at stroke, age at examination, and time since stroke.

participant demographics are illustrated in Table 1, where SD denotes Standard Deviation. Fig. 1 shows the age distribution at examination of control and stroke cases and additionally for every subject in the stroke cohort the age at stroke and time between stroke and imaging. Subject No.15 (control), No.17 (stroke), and No.21 (stroke) were excluded, due to technical issues during acquisition. During the preprocessing phase three stroke Subjects (No.3, 10 and 22) and control Subjects (No.26, 33 and 34) were excluded because of high motion artefacts and severe stroke (more than the half of the size of a hemisphere was affected). The stroke events occurred at different spatial locations on the right (RH) or left hemisphere (LH). The children were right-, left- or mixed handed. The time frame between scan event and stroke event, as well as the range of the age at stroke of the children ranges from 0 to 15 years. All participants' guardians (parents) were informed about the aim of the study and gave their written, informed consent prior to inclusion. The protocol of this study was approved by the Ethics Committee of the Medical University of Vienna and performed in accordance with the Declaration of Helsinki (1964), including current revisions and the EC-GCP guidelines. The scanning was performed on a 3T TIM Trio

Table 1: Participant demographics

	control	pediatric stroke
Sample size	16 (7 female)	16 (5 female)
Excluded	4	5
Mean age, yr (SD)	11.2 (3.19)	11.63 (3.14)
Stroke location (number of subjects)	-	RH (7), LH (7), RH+LH (2)

System (Siemens Medical Solution, Erlangen, Germany) Scanner and rs-fMRI measurements were performed using single-shot, gradient-recalled, echo-planar imaging with the following setup: TR = 2000 ms, TE = 42 ms, FOV = 210 x 210 mm, slices = 20, gap between slices = 1 mm, slice thickness = 4 mm, frames = 150 volumes. All subjects are scanned in an awake state with open eyes for 5 minutes. To restrict head motion, pillows are used as fixation on both

sides of the child's head. The probands wore headphones to attenuate the noise level during scan. All study participants watched a video, explicitly designed for children, which showed and explained an MRI acquisition procedure.

Anatomical and Functional Preprocessing: Anatomical and functional preprocessing is performed using Freesurfer[1][6] and FSL[2][10]. The anatomical image preprocessing pipeline includes motion correction, intensity correction, normalisation to MNI305 standard space, skull stripping, automatic subcortical segmentation, White Matter (WM) segmentation, surface tesselation and smoothing (standardized meshspace). The functional preprocessing includes a registration to the anatomical data, slice-timing correction, head motion regression and bandpass temporal filtering (0.01 - 0.1 Hz) to remove constant offsets and linear trends. Cerebral signals of the stroke and control cases are resampled to common FreeSurfer fsaverage5 space [7]. After this alignment every subject's cortical surface is represented as a standardized mesh consisting of 20484 nodes. After resampling the data are spatially smoothed using a 4 mm FWHM Gaussian filter. To obtain comparability between subjects all measurements described in this section are performed on this standardized representation.

Group Analysis and Correlation Measures: For the identification of correlating regions, the Pearson correlation coefficient is computed between the time course of a node $x(t)_i$ in each subject's brain and every other node's $x(t)_j$ time course. This results in a $N \times N$ correlation coefficient Matrix $CM_{i,j}$, expressed in Equation 1, where N is the number of nodes observed, i the ith row and j the jth column of the matrix, t the time frame and $\bar{x_i}$,$\bar{x_j}$ the average activity intensity across all of the time points at position i and j [14].

$$CM_{ij} = \frac{\sum[(x(t)_i - \bar{x_i})(x(t)_j - \bar{x_j}]}{\sqrt{\sum[(x(t_i - \bar{x_i})^2 (x(t_j) - \bar{x_j})^2]}} \tag{1}$$

Assessing long- and short range connectivity patterns over time: The degree value D_i used in this work is a network measure which enumerates the number of edges connected to a node i. For its computation we represent all brain surface voxels as nodes in a graph, with edges connecting pairs of nodes with a positive signal correlation above a threshold. First, the CM is used to extract node pairs with a correlation above a threshold of 0.4, and the degree is computed using the Brain Connectivity Toolbox (BCT) [13] (Equation 2):

$$D_i = \sum d_{ij}, i, j = 1 \ldots N, i \neq j. \tag{2}$$

We use the distance between two connected nodes to define long and short range connections, similar to [5, 15, 14] and compare their characteristics in the stroke- and control cohort. To establish an age independent definition of long and short range, we use the Euclidean distance E_{ij} between the coordinates of connected

[1] http://surfer.nmr.mgh.harvard.edu, [accessed 21^{st} August 2016]
[2] http://fsl.fmrib.ox.ac.uk/fsl/fslwiki/FSL, [accessed 21^{st} August 2016]

nodes on the fsaverage5 surface. For the analysis a neighbourhood Q of ≤ 15 mm is defined for short-range (SR) and > 15 mm for long-range (LR) connectivity. Since these limits match for the adult brain a normalized representation of the data on a fsaverage5 brain is required. Finally, following Sepulcre et al. [14], we evaluate the ratio R between the number of short-range and the number of all connections to correlating nodes, to be able to express relationships between the appearance and disappearance of these connectivity types over time (cf. Equation 3).

$$R_i = \frac{\sum_{j=1}^{n} (E_{ij} \leq Q_{SR})}{\sum_{j=1}^{n} E_{ij}}, i = 1, \ldots, N \tag{3}$$

3 Results

We analyse two aspects of the development, and for each we compare control- and stroke cohorts. First we assess the short and long range functional connectivity, and the development of this ratio during maturation. We test whether there are regions in which this ratio is different in individuals affected by stroke. Secondly, we compare the overall degree characteristics of cortical points in the two cohorts.

Analysis of short and long range connectivity during maturation*. Long and short range characteristics of the functional connectivity in the child's healthy brain showed an evolving towards the characteristic of the adult brain but contrary traits in the case of the developing brain affected by stroke:* We compare the development of SR and LR connectivity in controls and stroke patients. In Fig. 2 for single subjects at age 8, 9 and 14 the mean LR (row 1 and 2) and the mean SR (row 3 and 4) connectivity of each node on the fsaverage 5 inflated brain surface are visualised. In both cohorts high SR connectivity is present in the superior part of the postcentral gyrus (primary somatosensory cortex), the precentral gyrus (primary motor cortex) and superior parietal part. In the control case these regions tend to increase in size from 8 to 14, which locations overlap with observation in the adult brain [14]. For stroke cases no longitudinal trend is observable. For the control group the posterior cingulum shows an increase and higher SR connectivity values (> 150) in comparison to stroke cases. In contrast to this, LR connectivities show a higher grade of variability compared to SR connectivity. This might reflect the link between their emergence and experience and learning processes over time, which vary among subjects. It could be a possible explanation of the higher grade of variability in LR compared to SR connectivity. The change of the ratio between SR and all connectivities is evaluated in 6 brain regions separately: Broca's Area (BA 44, BA 45), Primary visual area (V1), Secondary visual area (V2) and Primary motor areas (BA 4a, BA 4p) anterior and posterior. In Fig. 3 the corresponding results are illustrated. Each subplot shows for one region the ratio of control and stroke cases for the RH and LH separately. In all regions, but with highest manifestation in the primary motor area a decrease of R over time is observable in the control cohort (except LH of BA 45 Broca Area). This can be interprated as a

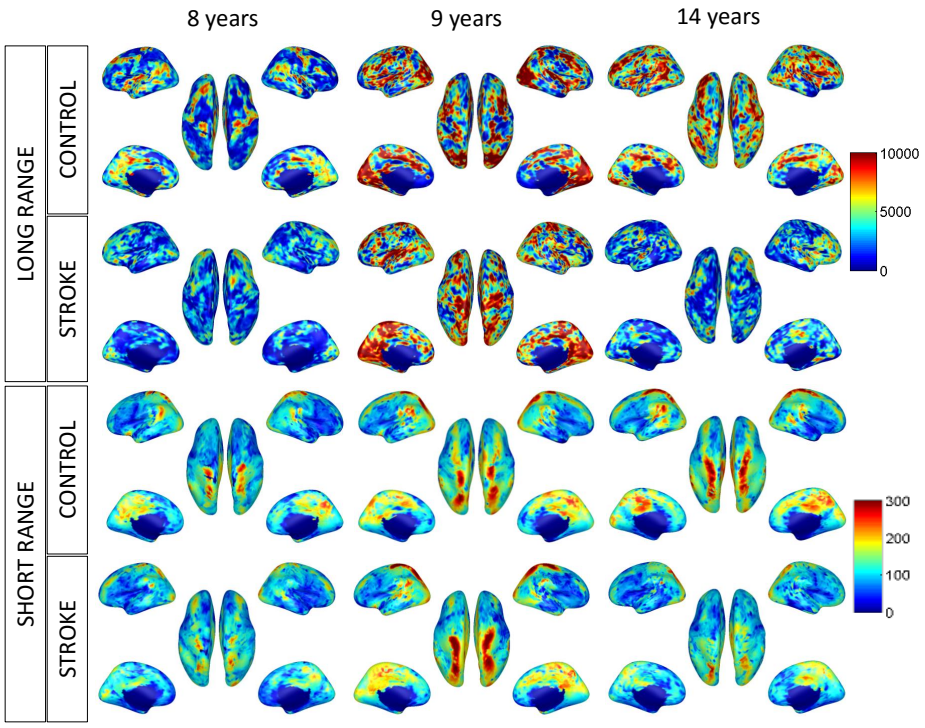

Fig. 2: Visualisation of long range (LR) and short range (SR) connectivity networks of single subjects in the control (c) and stroke (s) cohort at age 8, 9 and 14 years.

decrease of SR connectivity on the one hand and an increase of LR connectivity on the other hand during ageing. These results correlate with the observation of Supekar et al. [15]. They report high local connectivity (neighbourhood of $\leq$ 14 mm) preferentially in regions with primary sensory and motor areas and distant cortical-cortical interaction in heteromodal association areas (neighbourhood $>$ 14 mm), in addition to a weakening of SR functional connectivity and strengthening of LR functional connectivity during childhood. For stroke cases we observed a contrary characteristic. In the Broca' Areas (BA 45) (areas associated with speech) we observed asymmetry between LH and RH in the control cohort. Fig. 4 visualises the slope difference between the control and stroke cohort of SR connectivity (a), LR connectivity (b) and ratio changes (c). Values are normalized according to the values of the control cohort. A higher change of the connectivity ratio for controls (positive slope difference of ratio connectivity between control and strokes) is observable in the corpus callosum, (the part of the brain which connects RH and LH) and superior motor area in both hemispheres. Asymmetric appearances of these differences are observable in the

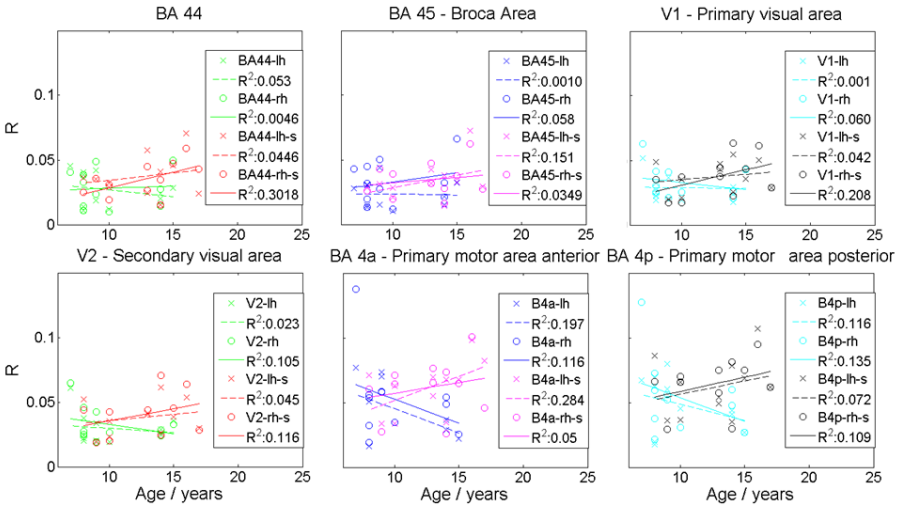

Fig. 3: Ratio development within the BA44 Broca's Area pars opercularis, BA45 Broca's Area pars triangularis, V1 primary visual area and V2 secondary visual area, BA 4 primary motor area anterior (a) and posterior (p). For every plot the ratio values for LH and RH for control and stroke (s) are visualised as well as the regression lines for these values with corresponding R^2 estimates.

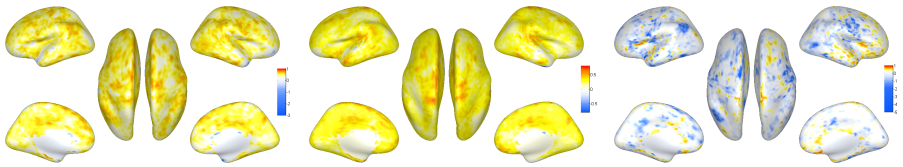

(a) LR connectivity (b) SR connectivity (c) Connectivity ratio

Fig. 4: Comparing control subjects and stroke patients: the difference of the slope for linear models of LR connectivity changes, SR connectivity changes, and ratio changes during ageing. Red areas indicate higher values for stroke patients, blue areas indicate higher values for control subjects.

temporal pole and the Broca's area pars triangularis, Broca's area pars opercularis and orbital frontal area of RH. In contrast to this for the stroke cohort the regions of higher changes of connectivity ratio (negative slope difference of ratio connectivity between control and strokes) appear asymmetrically: In the LH the posterior cingular cortex in the limbic lobe is observable, which is involved in processing, learning and memory tasks as well as in the formation of emotion. It also forms a central node in the Default Mode Network (DMN) [4]. The supra

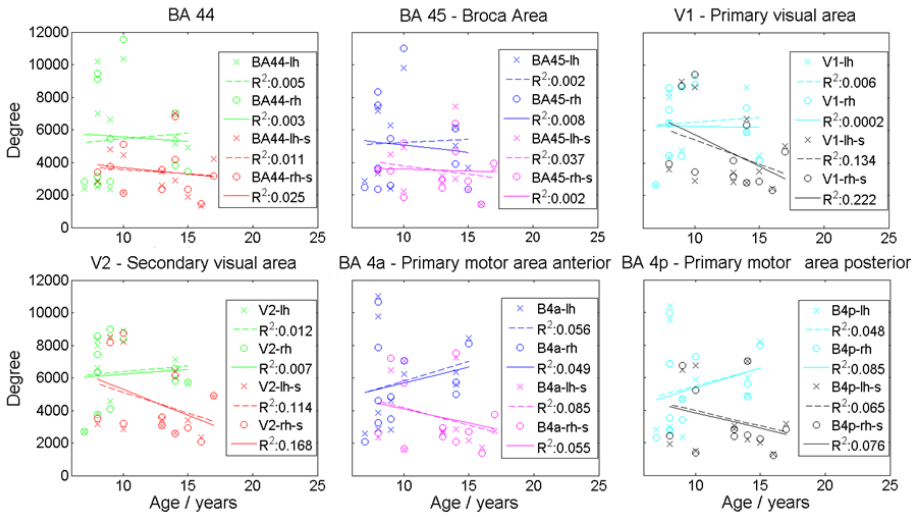

Fig. 5: Degree development within the BA44 Broca's Area pars opercularis, BA45 Broca's Area pars triangularis, V1 primary visual area and V2 secondary visual area, BA 4 primary motor area anterior (a) and posterior (p). For every plot the degree values for LH and RH for control and stroke (s) are visualised as well as the regression lines for these values with corresponding R^2 estimates.

marginal area shows higher changes of the connectivity ratio in stroke cases, which plays an important role in the perception of language. In the RH higher slope changes for stroke lie in the inferior parts of post (primary somatosensory area) and precentral areas (primary motor area).

Analysis of degree distribution during maturation. *With increasing age in the healthy brain an increase of degree and the emergence of specialised network nodes is observable, whereas the brain affected by stroke shows a decrease in degree:* We measure age dependent changes of the average degree distribution for the same brain regions. The graph based representation of the fsaverage 5 surface consist of 20484 nodes, 10242 for every hemisphere. The degree is only estimated between correlating nodes (> 0.4). In Fig. 5 the corresponding results are illustrated. Each sub plot shows for one region the degree of control and stroke cases for the RH and LH separately over the age. The control cases exhibit higher degree compared to stroke cases on average. In the healthy cohort at age between 7 and 8 the nodes of degree 5000 are located in the distant poles of the brain (frontal and occipital pole), where in contrast to this primary motoric centers show nodes of degree < 2500. With increasing age more specialised spots of nodes with degree > 10000 are observable, which correlates with an increase of degree over age in Fig. 5. In the stroke case a contrary behaviour is observable.

4 Conclusion

In this paper we report initial results analysing the changing functional connectivity in the child's developing brain after ischaemic stroke. The analysis is based on a graph analysis of functional networks to capture developmental traits of short and long range connectivity changes during maturation towards characteristic of the adult brain observed by [14]. In our initial results, stroke patients exhibit a development in the ratio of short and long range connectivity, and degree substantially different from control subjects. We observed a stronger change of short/long range connectivity ratio after stroke in regions involved in the evolving default mode network compared to healthy brains, where the DMN develops over time, starting from subtle connections in childhood [5]. Our initial results indicate asymmetric differences between control subjects and stroke patients of the development of the connectivity ratio in regions involved in speech perception. The one-sided-lateralization for language is evident in infancy and increases with age [17][9], and might be linked to these findings.
The current results present initial findings and valid statements require additional analysis and experiments. The location of stroke appearance and size varies across patients in this study, which limits our approach. Also the age at stroke and the time since stroke vary among the study population. Thus, we focused on deriving general trends of functional connectivity over age and not subject specific characteristics or stroke specific influences. Our findings demonstrate the feasibility and value of functional network analysis in the developing brain.

Acknowledgement

This work was co-funded by the Oesterreichische Nationalbank (Anniversary Fund, project number 15356), by the FWF under KLI 544-B27 and I 2714-B31, by the European Commission FP7-PEOPLE-2013-IAPP 610872 and by ZIT Life Sciences 2014 (1207843).

References

1. N.R. Altman and B. Bernal. Clinical applications of functional magnetic resonance imaging. *Pediatric Radiology*, 45(3):382–396, 2015.
2. V. Anderson, M. Spencer-Smith, and A. Wood. Do children really recover better? Neurobehavioural plasticity after early brain insult. *Brain : a journal of neurology*, 134(Pt 8):2197–221, aug 2011.
3. B. Casey, N. Tottenham, C. Liston, and S. Durston. Imaging the developing brain: what have we learned about cognitive development? *Trends in Cognitive Sciences*, 9(3):104–110, 2005.
4. D.A. Fair, A.L. Cohen, N.U.F. Dosenbach, J.A. Church, F.M. Miezin, D.M. Barch, M.E. Raichle, S.E. Petersen, and B.L. Schlaggar. The maturing architecture of the brain's default network. *Proceedings of the National Academy of Sciences of the United States of America*, 105(10):4028–32, mar 2008.

5. D.A. Fair, A.L. Cohen, J.D. Power, N.U.F. Dosenbach, J.A. Church, F.M. Miezin, B.L. Schlaggar, and S.E. Petersen. Functional brain networks develop from a "local to distributed" organization. *PLoS computational biology*, 5(5):e1000381, may 2009.
6. B. Fischl. FreeSurfer. *Neuroimage*, 62(2):774–81, August 2012.
7. B. Fischl, M.I. Sereno, R.B. Tootell, and A.M. Dale. High-resolution intersubject averaging and a coordinate system for the cortical surface. *Human brain mapping*, 8(4):272–84, 1999.
8. E.M. Gordon, P.S. Lee, J.M. Maisog, J. Foss-Feig, M.E. Billington, J. Vanmeter, and C.J. Vaidya. Strength of default mode resting-state connectivity relates to white matter integrity in children. *Developmental science*, 14(4):738–51, jul 2011.
9. M.A. Groen, A.J.O. Whitehouse, N.A. Badcock, and D.V.M. Bishop. Does cerebral lateralization develop? A study using functional transcranial Doppler ultrasound assessing lateralization for language production and visuospatial memory. *Brain and behavior*, 2(3):256–69, may 2012.
10. M. Jenkinson, C.F. Beckmann, T.E.J. Behrens, M.W. Woolrich, and S.M. Smith. FSL. *NeuroImage*, 62(2):782–90, aug 2012.
11. S. Kornfeld, J.A. Delgado Rodríguez, R. Everts, A. Kaelin-Lang, R. Wiest, C. Weisstanner, P. Mordasini, M. Steinlin, and S. Grunt. Cortical reorganisation of cerebral networks after childhood stroke: impact on outcome. *BMC neurology*, 15(1):90, jan 2015.
12. P. K. Kuhl. Brain Mechanisms in Early Language Acquisition. *Neuron*, 67(5):713–727, September 2010.
13. M. Rubinov and O. Sporns. Complex network measures of brain connectivity: uses and interpretations. *NeuroImage*, 52(3):1059–69, 2010.
14. J. Sepulcre, H. Liu, T. Talukdar, I. Martincorena, B.T. Thomas Yeo, and R.L. Buckner. The organization of local and distant functional connectivity in the human brain. *PLoS Computational Biology*, 6(6):1–15, 2010.
15. K. Supekar, M. Musen, and V. Menon. Development of large-scale functional brain networks in children. *PLoS biology*, 7(7):e1000157, jul 2009.
16. M.E. Thomason, E.L. Dennis, A.A. Joshi, S.H. Joshi, I.D. Dinov, C. Chang, M.L. Henry, R.F. Johnson, P.M. Thompson, A.W. Toga, G.H. Glover, J.D. Van Horn, and I.H. Gotlib. Resting-state fMRI can reliably map neural networks in children. *NeuroImage*, 55(1):165–75, mar 2011.
17. D. Wang, R.L. Buckner, and H. Liu. Functional Specialization in the Human Brain Estimated By Intrinsic Hemispheric Interaction. *Journal of Neuroscience*, 34(37):12341–12352, 2014.